



The Study of Interference Effect for Cascaded Diffuser Augmented Wind Turbines

Sheng-Huan Wang¹ and Shih-Hsiung Chen²

¹ Engineer, Department of Research and Development, Jetpro Technology, Inc.
701, 11F, No. 1-57, Chung-Hwa Road, Yong-Kang City, Tainan County, Taiwan
huan@jetprotech.com.tw

² General Manager, Jetpro Technology, Inc.
701, 11F, No. 1-57, Chung-Hwa Road, Yong-Kang City, Tainan County, Taiwan
shchen86@hotmail.com

ABSTRACT

The diffuser augmented wind turbine (DAWT) (or so called ducted wind turbine) was believed to have a good wind power energy conversion effect. By using a cascading arrangement the wind turbines could be installed closely, resulting in is an economy of land, space and money. However, few studies have been conducted on the influence of cascaded diffuser augmented wind turbines on the integral efficiency. The aim of this study, therefore, investigates the interference effect for cascaded diffuser augmented wind turbines. In this study two rated capacities of 200 W diffuser augmented wind turbines are adopted as experimental models and set up in the test section of the wind tunnel. The power outputs of the wind turbines are measured at various crosswind degrees with the different distances between the two yawing centers of the wind turbines. Results show that when the crosswind is less 45 degrees, the interference effect can be low and the power outputs have very little to do with the distance between the two yawing centers of the wind turbines. To conclude, this study may be of importance in explaining the interference between the two wind turbines, as well as in providing engineers with a better understanding of how to install cascaded wind turbines effectually.

KEYWORDS: DAWT, CASCADED WIND TURBINES, INTERFERENCE EFFECT

Introduction

By means of optimal aerodynamic design, all kinds of wind turbines have been improved. In particular, the power coefficient of the traditional 3-bladed propeller type wind turbine could be raised to about 0.4. There are some defects, however, including the high noise level and high cut-in wind speed that make it difficult to raise the performance. Comparatively, it was realized that a ducted wind turbine design has aerodynamic advantages over traditional propeller type turbines in converting wind energy to electric power. By creating a field of low pressure behind an appropriate duct, the wind is accelerated through the turbine blades and carries more dynamic energy. That is to say the power corresponds to wind velocity raised to the third power. Furthermore, the duct can limit the tip vortex generation, reduce the tip loss and lower noise levels. At a constant wind speed we only need a smaller blade diameter to generate the same power in comparison to the traditional 3-bladed propeller type wind turbine.

Kogan and Nissim (1962) and Kogan and Seginer (1963) first referred to a wind turbine with convergent entrance and divergent exit that could reduce the cut-in speed. In their experiment, when the ratio of the duct length to the minimum duct diameter was 7 to 1 and the drag coefficient of the duct was between 0.18 and 0.22, a higher efficiency was

presented. After Kogan et al., Igra (1976) did a series of experiments extending previous reach by adopting standard airfoil (NACA4412) as the sectional profile of the duct and putting emphasis on the change of the pressure gradient at the diffuser exit. The results showed that the pressure at the diffuser exit could be reduced by adding a few ringshaped airfoils around it and the efficiency was raised to 52%.

As the energy crisis lessened, the development of wind energy became tardier. Over the last few decades, there has been a dramatic decrease in the number of publication on ducted wind turbines. Researchers didn't take wind energy seriously until oil shortages and global climate changes raised interest in the development of renewable energy sources.

Frankovic and Vrsalovic (2001) estimated that the efficiency of the ducted wind turbine could be raised 3.5 times while the area of the inlet was 3 times of the minimum section. Numerical investigations are carried out for flow fields around flanged diffusers to develop small-type wind turbines under 1.5 kW by Abe and Ohya (2004). In their calculations, an advanced closure approximation is adopted, within the framework of non-linear eddy-viscosity modeling, which aims specifically at an improved representation of turbulence anisotropy. The study shows that the performance of a flanged diffuser strongly depends on the loading coefficient as well as the opening angle because it greatly affects the nature of the separation appearing inside the diffuser. Abe and Ohya et al. (2005) measured the mean velocity profiles behind a wind turbine by using a hot-wire technique. Characteristic values of the flow fields were estimated and compared with those for a bare wind turbine. In particular, a considerable difference was seen in the destruction process of the tip vortex between the bare wind turbine and the wind turbine with a flanged diffuser. Wang and Chen (2008) suggested that increasing the number of blades effectively causes the lower cut-in wind speed and the higher power coefficient. But more blades lead to more blockage and lower blade entrance velocity. Eventually the power coefficient will be reduced.

Until recently, most research has placed emphasis on how the ducted wind turbine transforms energy effectively; literature on the interference effect for cascaded diffuser augmented wind turbines is still lacking. As windfarm development has increased over the past decade, a lot of research has been done to estimate the overall performance of windfarms. Rados et al. (2001) compare the performance of six wake models in offshore windfarm environments. The study found that almost all of the models overestimate the wake effects. There were also significant inconsistencies between the model predictions that appeared in the near wake and turbulence intensity results. Based on the conclusions of that study, a number of modifications to the original models have already been implemented. Clearly, some of the previous model discrepancies have been corrected and the overall performance improved.

The aerodynamic interaction between two rotors in both axial and yawed wind conditions has been simulated using the Vorticity Transport Model by Fletcher and Brown (2009). The aerodynamic interaction is a function of the tip speed ratio, the separation between the rotors, and the angle of yaw to the incident wind. The simulations show that the momentum deficit at a turbine operating within the wake developed by the rotor of a second turbine can substantially limit the mean power coefficient that can be developed by the turbine rotor.

As mentioned above, the traditional propeller type has a strong interference effect between neighboring turbines; therefore, they need to be installed far apart at roughly 5 diameters or more. Ducted wind turbines, on the other hand, should have less interference between neighboring wind turbines because the duct plays some kind of role to have the main flow field contained inside the duct. Therefore more ducted wind turbines can be installed in the limited wind farm and more power is available. As a result, the major purpose of the present study is to investigate the interference effect between neighboring wind turbines. Two rated outputs of 200 W ducted wind turbines (JPS-200) made by Jetpro Technology, Inc. were

adopted as the experimental models. They were set up side by side in the test section of the open low-speed wind tunnel. The power outputs of the wind turbines are measured at various crosswind degrees with different distances between the two yawing centers of the wind turbines. The findings show that the larger crosswind degrees and the closer distances between neighboring turbines contribute to the drop in the performance of the cascaded diffuser augmented wind turbines.

Experimental Facility and Method

Wind Tunnel and Wind Turbine Models Setup

In this study the wind tunnel is an open low-speed tunnel. A schematic drawing is shown in Figure 1. There are four axial fans driven by four 20 Hp inverter duty motors to provide the requisite wind source. For inlet flow turbulence control and to eliminate swirl, one honeycomb is included in the middle position of the straightener which is 4.8 m by 4.8 m and 4.8 m in length. A 1.77 to 1 contraction ratio follows the straightener to accelerate the flow and reduce the boundary layer thickness. The straight section contributes enough space to lower turbulence intensity. Furthermore, the 2.5 m by 2.5 m jet section accelerates the flow again. A potential flow field is constituted in the downstream of the wind tunnel exit. To ensure that the flow is uniform in this area the wind turbine models are set up at a 1 meter distance from the wind tunnel exit.

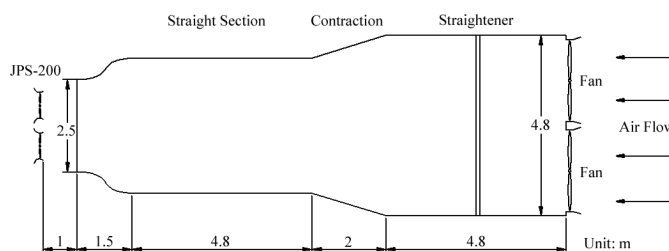


Figure 1: Schematic Drawing of Wind Tunnel and Wind Turbine Models Setup

Wind Turbine Models

Jetpro Technology, Inc. JPS-200 (Figure 2) is adopted as a wind turbine model. The duct is 0.25 meters in length with the convergent inlet and divergent exit. The diameter of the inlet is 0.74 meters, the exit is 0.9 meters and the minimum section is 0.7 meters. The throat is located 0.3 meters distance from the inlet of the duct, i.e. 30 % length of the duct. A converged inlet duct for accelerating wind speed, thus causing higher dynamic pressure over the turbine blades, is incorporated with a diverged tail section for adjusting the turbine exit pressure to achieve higher power output and lower cut-in wind speed. Additionally, the duct geometry provides the movement for free yawing motion with the various wind direction.

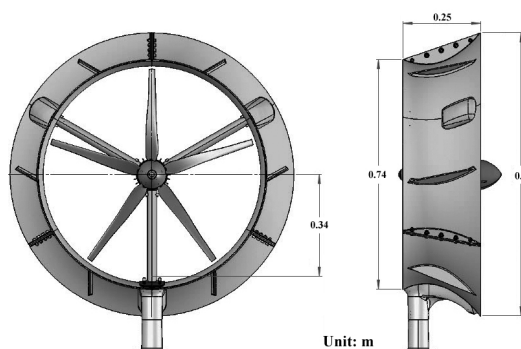


Figure 2: The Overall Wind Turbine JPS-200

Flow Velocity Measurements

A Pitot tube is mounted on the center of the test section (i.e. at 1 meter distance from the wind tunnel exit) and connected to the MODUS DT low differential pressure transmitter, giving the free stream dynamic pressure reading on the test section. The MODUS model DT-1-05P-0-10L has a range of 250 Pa and a transmitter accuracy of $\pm 1\%$ of span. By applying Bernoulli's principle free stream velocities can be calculated. Free stream velocities in this wind tunnel can range from 2 m/s to 15 m/s via four axial fans driven by four 20 Hp inverter duty motors.

Wind Turbine Power Measurements

For the purpose of energy storage, the alternating current from a generator of a small wind turbine should be transformed into the direct current. Figure 3 shows a schematic of the power measurements, which consists of a battery, a data acquisition (DAQ) model, a personal computer, two electric current meters, two voltage meters and two charge controllers. For each the duct wind turbine the electric current flows into the charge controller that can raise and stabilize the voltage and limit the electric current, and then flows into the battery. In this study the 100 Ah capacity of the battery was adopted as a load. The electric currents and voltages were measured individually between the charge controller and the battery. NI USB-6009 was used to log data from the electric current and voltage meter and was saved on the personal computer from the current meter. From the experimental data, power outputs are calculated by multiplying the voltage and current.

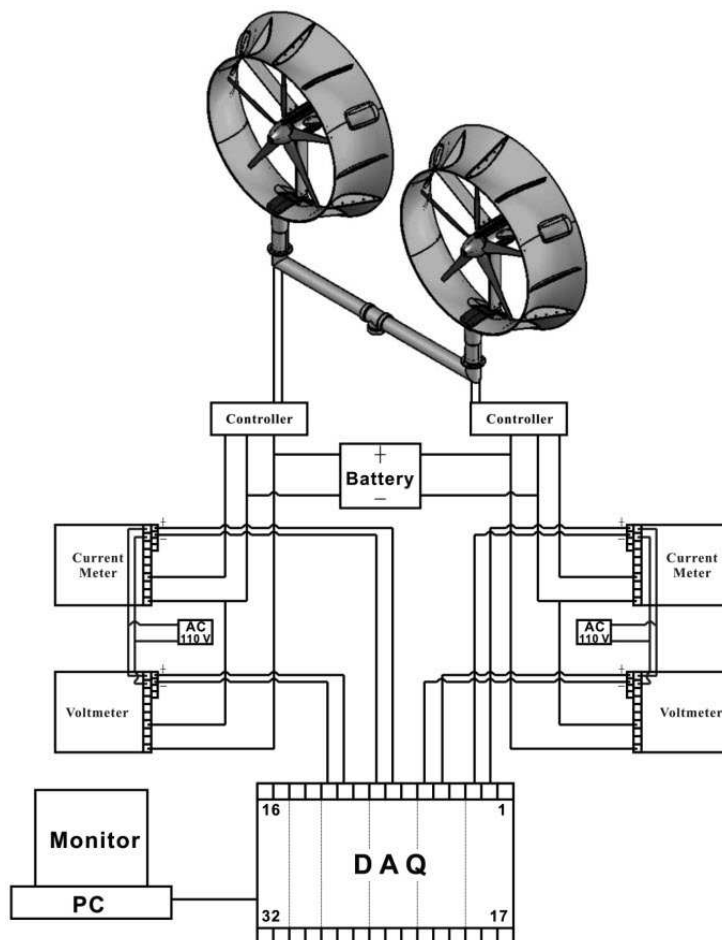


Figure 3: Schematic View of the Power Measurements

Test Condition

As shown in Figure 4, two wind turbine models were settled in the test section of the open low-speed wind tunnel. In three cases, the distance between the center yaw centers of neighboring wind turbines were set up $D_{YC}/D_D=1.22$ 、 1.44 and 1.67 and then the power outputs were measured at seven different crosswind degrees from 0 to 90.

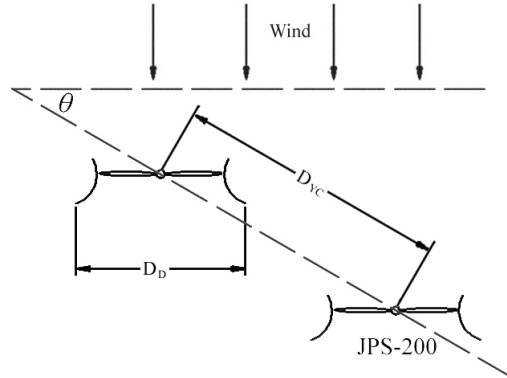


Figure 4: Schematic Drawing of Wind Tunnel and Wind Turbine Models Setup

Experimental Results and Discussions

The power curve of the JPS-200 ducted wind turbine is shown in Figure 5. The 200 W rated power is output at 12 m/s rated wind speed. In the high wind speed region we see that the power curve appears to be consistent with the cubic curve of the wind speed, but in the low wind speed region the power is lower than the theoretical value. This may be due to the lower efficiency of the generator when working at a low rotating speed. For this reason the ratio of power coefficient (C_p/C_{p0}) is adopted in this study to present the interference effect for cascaded diffuser augmented wind turbines. The power coefficient is defined as the Eq. (1) and the subscript 0 means the single wind turbine.

$$C_p = \frac{P}{\frac{1}{2} \rho \pi R^2 V_\infty^3} \quad (1)$$

C_p : Power Coefficient

P : Power Output

R : Rotor Radius

ρ : Air Density

V_∞ : Wind Velocity

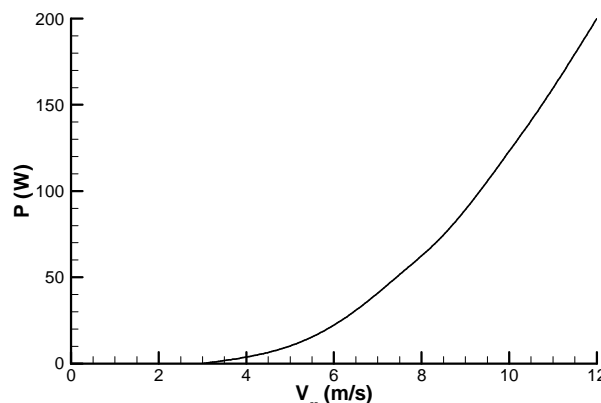


Figure 5: Power Curve of JPS-200 Ducted Wind Turbine

The influences of crosswind on the ratio of power coefficient at $D_{YC}/D_D=1.22$ are presented in Figure 6 and Figure 7. The ratios of power coefficient of the upstream wind turbine drop with the increasing angle of crosswind and maximum range is about 0.1, i.e. 10% power loss. The major causes of the power loss are that the blockage effect of the downstream wind turbine leads to the decreasing mass flow rate into the upstream wind turbine. In Figure 7 there are slight variations in the power coefficient of the downstream wind turbine under 45 degrees crosswind. At 60 degrees crosswind C_p/C_{p0} raises from 0.5 to 0.8 with the increasing wind speed, i.e. 50% power loss at lower wind speed and 20% power loss at rated wind speed. As crosswind raises to 75 degrees the cut-in wind speed begins to lag behind $V_\infty/V_{rated}=0.46$ and the rated power loss is 90%. Finally, at 90 degrees crosswind the cut-in wind speed reaches to $V_\infty/V_{rated}=0.77$ and the rated power loss is 95%

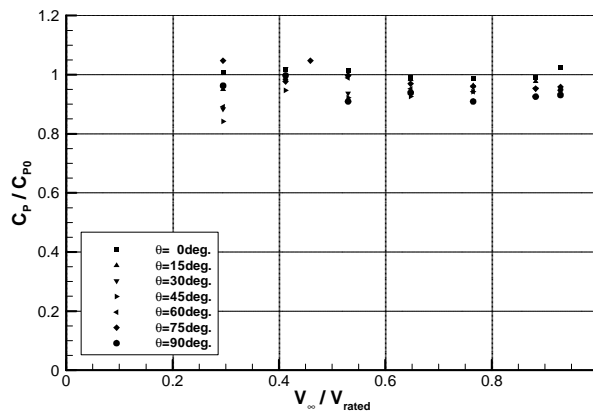


Figure 6: The Ratio of Power Coefficient of the Upstream Wind Turbine at $D_{YC}/D_D=1.22$

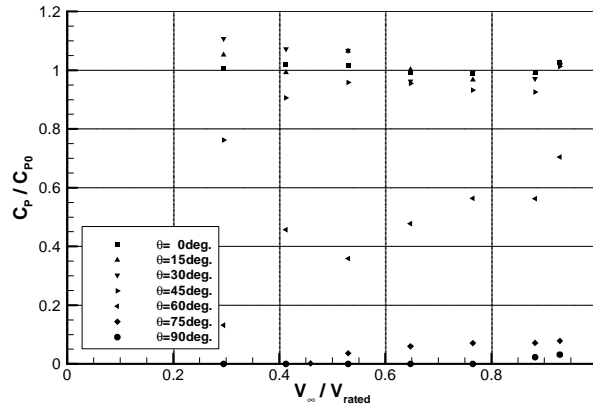


Figure 7: The Ratio of Power Coefficient of the Downstream Wind Turbine at $D_{YC}/D_D=1.22$

The influences of crosswind on the ratio of power coefficient at $D_{YC}/D_D=1.44$ are presented in Figure 8 and Figure 9. The ratios of power coefficient of the upstream wind turbine drop with the increasing angle of crosswind and maximum range is about 0.1, i.e. 10% power loss. In Figure 9 there are slight variations in the power coefficient of the downstream wind turbine under 45 degrees crosswind. At 60 degrees crosswind C_p/C_{p0} raises from 0.5 to 0.9 with the increasing wind speed, i.e. 50% power loss at lower wind speed and 10% power loss at rated wind speed. As crosswind raises to 75 degrees the cut-in wind speed begins to lag behind $V_\infty/V_{rated}=0.46$ and the rated power loss is 90%. Finally, at 90 degrees crosswind the cut-in wind speed reaches to $V_\infty/V_{rated}=0.77$ and the rated power loss is 95%.

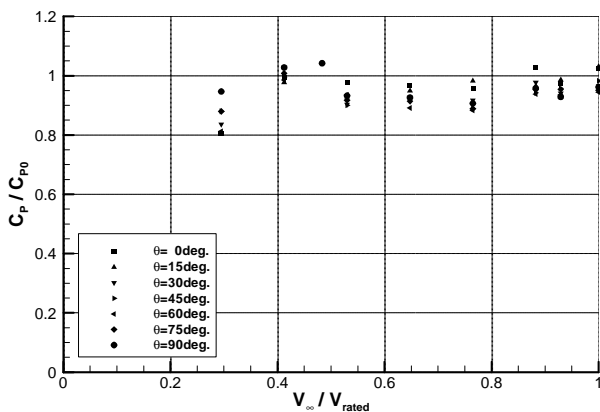


Figure 8: The Ratio of Power Coefficient of the Upstream Wind Turbine at $D_{YC}/D_D=1.44$

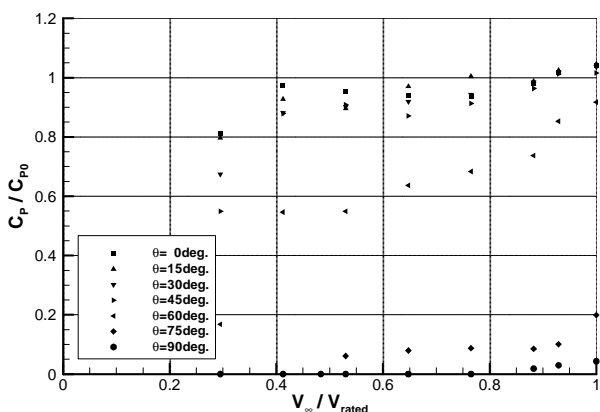


Figure 9: The Ratio of Power Coefficient of the Downstream Wind Turbine at $D_{YC}/D_D=1.44$

The influences of crosswind on the ratio of power coefficient at $D_{YC}/D_D=1.67$ are presented in Figure 10 and Figure 11. The ratios of power coefficient of the upstream wind turbine drop with the increasing angle of crosswind and maximum range is about 0.1, i.e. 10% power loss. In Figure 11 there are slight variations in the power coefficient of the downstream wind turbine under 45 degrees crosswind. At 60 degrees crosswind C_p / C_{p0} raises from 0.6 to 1 with the increasing wind speed, i.e. 40% power loss at lower wind speed and approximately no power loss at rated wind speed. As crosswind raises to 75 degrees the cut-in wind speed maintains $V_{\infty}/V_{rated}=0.25$ and the rated power loss is 50%. Finally, at 90 degrees crosswind the cut-in wind speed reaches to $V_{\infty}/V_{rated}=0.77$ and the rated power loss is 95%.

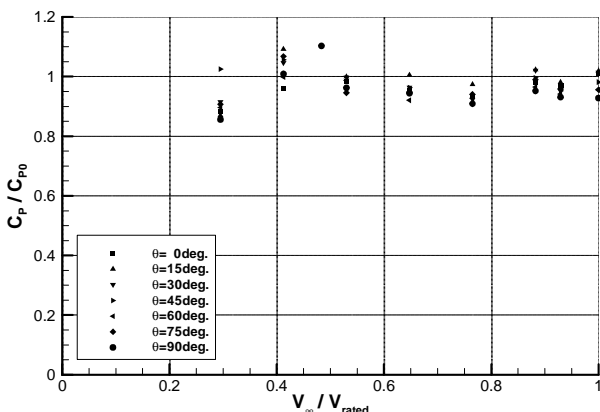


Figure 10: The Ratio of Power Coefficient of the Upstream Wind Turbine at $D_{YC}/D_D=1.67$

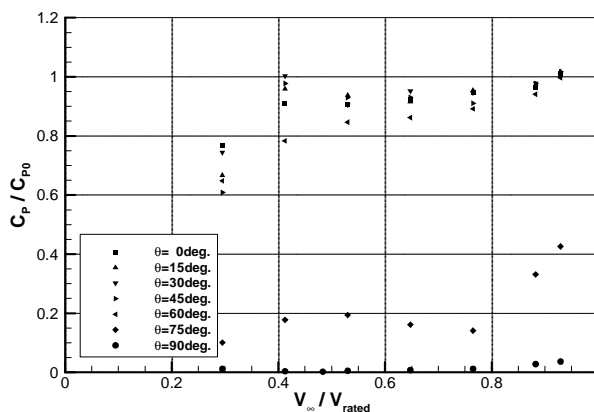


Figure 11: The Ratio of Power Coefficient of the Downstream Wind Turbine at $D_{YC}/D_D=1.67$

Since the opening wind tunnel is used in this study, the environmental turbulence influences the flow field of the test section at low wind speed. The experimental results show that the larger errors occur in the low wind speed region. Furthermore, a small variation in performance between two JPS-200 wind turbines results from fabrication.

As observed in Figure 12, when the crosswind is less than 45 degrees, the influence of the distance between the two yawing centers of the wind turbines on the ratio of power coefficient is powerless. When the crosswind is larger than 45 degrees, the ratio of power coefficient drops drastically with the increasing angle of crosswind and the values become lower and lower with the decreasing D_{YC}/D_D . These results are attributable to that the closer distance between the two wind turbines, which leads to a large overlap between the two wind turbines at the same angle of crosswind turbines, i.e. the downstream wind turbine works within the wider region of wakes. Finally, the crosswind reaches 90 degrees; therefore, the downstream wind turbine works within the full region of wakes. For this reason approximate zero power outputs from the downstream wind turbine and the ratios of power coefficient are about 0.5.

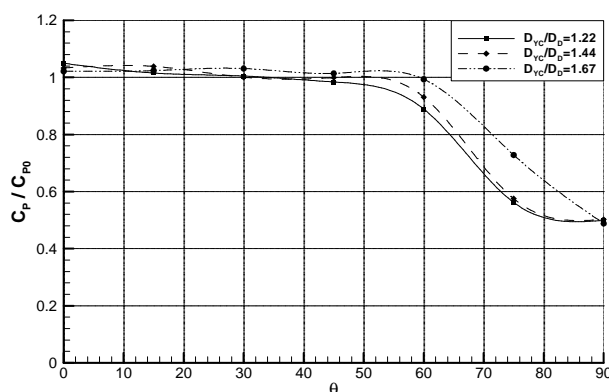


Figure 12: The Influence of Crosswind on the Ratio of Power Coefficient at Various D_{YC}/D_D

Conclusions

When the crosswind is less than 45 degrees, loss of total power outputs are slight with increasing angles of crosswinds and the ratios of power coefficient have very little to do with the distance between the two yawing centers of the wind turbines. When the crosswind is larger than 45 degrees, the cut-in wind speed of the downstream wind turbine becomes higher and the ratios of power coefficient drop rapidly with the decreasing D_{YC}/D_D . The results show that the ducted wind turbines can work in the region of 180 degrees by adopting a closely

cascading arrangement. Although the working region is narrower, the capacity of the installed wind turbine increases. Furthermore, the ducted wind turbines can work in the region of 240 degrees by adopting a sparsely cascading arrangement, although the capacity of the installed wind turbine will decrease. Therefore this study details how to install cascading wind turbines that will work efficiently. By using a closely cascading arrangement in the seasonal windfarm the capacity can be raised. Furthermore, by using a sparsely cascading arrangement in the unsteady windfarm the working region can be extended.

Acknowledgments

This study was supported by Jetpro Technology, Inc. Their financial and technical supports are acknowledged.

References

- Kogan, A., and Nissim, E. (1962), "Shrouded Aerogenerator Design Study, Two-Dimensional Shroud Performance", Bulletin of the Research Council of Israel, Vol. 11, pp. 67-88.
- Kogan, A., and Seginer, A. (1963), "Shrouded Aerogenerator Design Study II, Axisymmetrical Shroud Performance", Proceedings of the Fifth Israel Annual Conference on Aviation and Astronautics, Israel.
- Igra, O. (1976), "Shrouds for Aerogenerators", AIAA Journal, Oct., pp. 1481-1483.
- Frankovic, B., and Vrsalovic, I. (2001), "New High Profitable Wind Turbines", Renewable Energy, Vol. 24, pp. 491-499.
- Abe, K. and Ohya, Y. (2004), "An Investigation of Flow Fields Around Flanged Diffusers Using CFD," Journal of Wind Engineering and Industrial Aerodynamics, Vol. 92, pp. 315-330.
- Abe, K., Nishida, M., Sakurai, A., Ohya, Y., Kihara, H., Wada, E., and Sato, K. (2005), "Experimental and Numerical Investigations of Flow Fields Behind a Small Wind Turbine with a Flanged Diffuser," Journal of Wind Engineering and Industrial Aerodynamics, Vol. 93, pp. 951-970.
- Sheng-Huan Wang and Shih-Hsiung Chen (2008), "Blade Number Effect for a Ducted Wind Turbine", Journal of Mechanical Science and Technology, Vol. 22, No. 10, pp. 1984-1992.
- K. Rados, G. Larsen, R. Barthelmie, W. Schlez, B. Lange, G. Schepers, T. Hegberg and M. Magnisson (2001), "Comparison of Wake Models with Data for Offshore Windfarms", Wind Energy, Vol. 25, No. 5, pp. 271-280.
- T. M. Fletcher and R. E. Brown (2009), "Simulating Wind Turbine Interactions Using the Vorticity Transport Model" 28th ASME Wind Energy Symposium.